Synthesis and characterization of nano-HA/PA66 composites

MEI HUANG*, JIANQING FENG, JIANXIN WANG, XINGDONG ZHANG
Engineering Research Center for Biomaterials, Sichuan University, Chengdu, China
Email: nic7500@scu.edu.cn

YUBAO LI, YONGGANG YAN
Institute of Materials Science and Technology, Analytical and Test Center, Sichuan University, Chengdu, China

Based on the bioactivity and biocompatibility of hydroxyapatite (HA) and the excellent mechanical performance of polyamide 66 (PA66), a composite of nanograde HA with PA66 was designed and fabricated to mimic the structure of biological bone which exhibits a composite of nanograde apatite crystals and natural polymer. The HA/PA66 composite combines the bioactivity of HA and the mechanical property of PA66. This study focused on the preparation method of HA/PA66 composite and the influence of HA crystals on the characterization of the composite. HA slurry was used directly to prepare HA/PA66 composite by a solution method, in which HA is able to form hydrogen bond, i.e. chemical bonding with PA66. The nano-HA needle-like crystals treated by hydrothermal method are better in the particle size distribution and the particle dispersion. The morphology, crystal structure and crystallinity as well as crystal size of these needle-like crystals are similar to bone apatite. The nano-HA needle-like crystals dispersed uniformly in PA66 matrix with reinforcement effect and can prevent the micro-crackle spreading into cleft and fracture during the deformation process. The mechanical testing shows that the nano-HA/PA66 composite has a good mechanical property, and may be a promising bone replacement material.

Introduction

HA [$Ca_{10}(PO_4)_6(OH)_2$] has been successfully applied in orthopedics as bone substitutes due to its excellent bioactivity and biocompatibility [1–3] which is probably from its similarity to the main mineral component in hard tissues of the body. Nevertheless, the fracture toughness of HA ceramics does not exceed $1\,MPa \cdot m^{1/2}$, as compared with $2–12\,MPa \cdot m^{1/2}$ for human bone [4, 5]. Therefore, the HA materials cannot be used as load-bearing implants, such as artificial teeth or long bones. These shortcomings greatly confine HA application as load-bearing biomaterials. How to improve the mechanical property of HA materials for hard tissue replacement is still an important issue for biomaterials science and engineering.

It may be possible to develop a synthetic substitute for bone in composite form, which is both mechanically compatible and biocompatible. If HA is utilized as reinforcing and active phase, the composite is potentially bioactive, i.e. bone bonding with bone becomes possible [6]. Composites for orthopedic applications have been designed with the aim of attempting to match the properties and structure of those of bone. These matrix materials were based on polyethlene [6–10], polyhydroxabutyrate [11, 12], as well as PLA, filled with synthetic HA particles.

PA66 is an important engineering plastic with excellent mechanical property, and it is also used as a medical polymer owing to its toughness, such as medical thread, artificial skin, etc. The degraded monomer of PA66, hexamethylene-diamine and hexanedioic acid, may have a role of anti-bacterium *in vivo* [13], but PA66 cannot form bone-bonding with bone tissue. Apatite is the main mineral part of calcified tissues [14, 15], the apatite crystals in bone are formed as thin needles, about 5–20 nm by 60 nm with a poor crystallinity in the collagen fiber matrix [10, 16], so bone can be considered as a polymer composite with nano-apatite reinforcement. HA is compounded with PA66 sufficiently, the composite could be also bioactive. Recently, the composite composed of nanograde apatite and PA66 was designed and prepared [17, 18]. In this study, a new fabrication method of HA/PA66 composite and the influence of HA crystals on the characterization of HA/PA66 were reported. This composite has excellent mechanical properties and bioactivity, and is a promising biomaterial for load-bearing bone replacement.

*Author to whom all correspondence should be addressed.

Materials and methods

Synthesis and hydrothermal treatment of HA

Analytical grade reagents $Ca(NO_3)_2$, $(NH_4)_2HPO_4$ and ammonia solution were used to synthesize HA. The solution of $(NH_4)_2HPO_4$ was slowly dropped into the stirred solution of $Ca(NO_3)_2$ at 50 °C, the pH was adjusted to 10–12 with ammonia solution. The as-received precipitate was washed with deionized water, and HA1 slurry was obtained. The HA1 slurry was processed hydrothermally in an autoclave at 140 °C, 3 bar for 2 h. After treatment, HA2 slurry was ready for preparing HA/PA66 composite [19, 20].

Preparation of HA/PA66 composite

PA66 with a molecular weight 18 000 (weight average molecular mass)(Asahi Chemical Industry Co. Ltd, Japan) was used for preparation of HA/PA66 composite. The amide solvent and HA1 slurry were put into the kettle, then the reactants were stirred and heated to disperse the particles of HA1 sufficiently and remove the water (> 100 °C). After the water was removed completely, PA66 was added into the solution, then went on heating and stirring until PA66 was dissolved absolutely. The solvent was drawn out by decompression distillation, the product was washed with hot deionized water and ethanol, and HA1/PA66 composite was obtained. HA2/PA66 composite was prepared with the same procedure. The weight ratio of HA to PA66 of both HA1/PA66 and HA2/PA66 composites was 50%.

HA/PA66 composites were smashed, vacuum dried, and prepared into the specimens of standard shape for mechanical testing using an injection-molding machine at 250–290 °C. The same preparation conditions were kept for HA1/PA66 and HA2/PA66 composite.

The particle sizes and distribution of two HA slurry were analyzed by laser particle analyzer (SL-1155, China). The phase composition and the crystal size of the HA and HA/PA66 were characterized by powder X-ray diffraction (XRD) (X'pert Pro MPD, Philip, The Netherlands) with Cu Ka (45 KV, 40 mA, graphite monochromators). The morphology of the HA crystals was observed using a transmission electron microscope (TEM) (JEOL, JEM-100CX, Japan). The mechanical properties of the HA/PA66 composite were measured with a universal-testing machine (Shimadzu, AG-10TA, Japan). Fracture surfaces were coated with gold films and observed using a scanning electron microscope (SEM) (Hitachi, S-450, Japan).

Results and discussion

Particle size distribution (PSD) and specific surface area of HA slurry

The particle size distribution and specific surface area of HA1 slurry (as-received precipitate without hydrothermal treatment) and HA2 slurry (with hydrothermal treatment) were analyzed using water as disperse medium. The results are listed in Table I. The data show that the particles sizes of two HA slurry were between nanometer and micrometer. The HA slurry is more suitable to form composite with PA66 to improve bonding strength between HA and PA66 because the nano-particles of HA slurry scatter in the PA matrix more uniformly than HA powder. The larger specific surface area i.e. the larger surface energy of the HA nano-particles is also favorable to make more contacting surface with PA66 matrix. As filler in a composite, the specific surface area and dimension of the filler is very important parameters to control the performance of composites. Their dimension and the specific surface areas show significant difference, which indicates that HA2 particles are smaller and the specific surface area is bigger than HA1.

TABLE I Particle size distribution and specific surface area of HA slurry

	HA1 slurry	HA2 slurry
Accumulate 10% diameter (μm)	0.10	0.09
Accumulate 50% diameter (μm)	0.55	0.44
Accumulate 90% diameter (μm)	1.71	0.97
Mean diameter (μm)	0.77	0.47
Specific surface area (m^2/cm^3)	16.0	19.3

TEM analysis

Fig. 1 is the TEM images of the HA slurry. In Fig. 1(b), it can be seen that HA2 crystals have excellent dispersion ability, presenting a needle-like morphology. The dimension of HA2 crystals is about 60–100 nm in length and 20–30 nm in diameter. In Fig. 1(a), HA1 crystals are imperfect and the crystallinity is lower, and the crystals have irregular morphology and exhibit sphere. Its particles are connected to each other and may be difficult to disperse well into the PA66 matrix.

X-ray diffraction analysis

Fig. 2 represents XRD pattern of HA1, HA2 and HA3 sintered products of HA2 at 1100 °C respectively. Quantitative analysis of XRD pattern indicated that HA3 is pure HA. From the result we can infer that HA1 and HA2 slurry are pure HA. As shown in Fig. 2, HA1 and HA2 have a poorly crystallized structure compared with sintered HA3, but HA2 exhibits relatively higher crystallinity than HA1 from the symmetry and the sharpness of the main HA characteristic peaks. XRD results prove that HA2 crystals are more perfect in crystalline structure after hydrothermal treatment than HA1. By measuring the half-height width of characteristic peak (0 0 2) of HA, the crystal dimension along c-axis was calculated with Sheer's equation. HA1 is 52 nm and HA2 is 68 nm approximately, which indicated that HA crystal grows along the c-axis direction during hydrothermal treatment [16], HA2 needle-like crystals are longer than HA1.

Fig. 3 is the XRD pattern of PA66 and HA/PA66 composites. It can be inferred that pure PA66 is alpha structure with relative high crystallinity from Fig. 3. In the HA/PA66 composites, the peak positions and conformation of HA1 and HA2 do not exhibit significant difference as compared with those in Fig. 2. This means the HA crystal structure did not change greatly during the process of composite preparation. However, the intensity

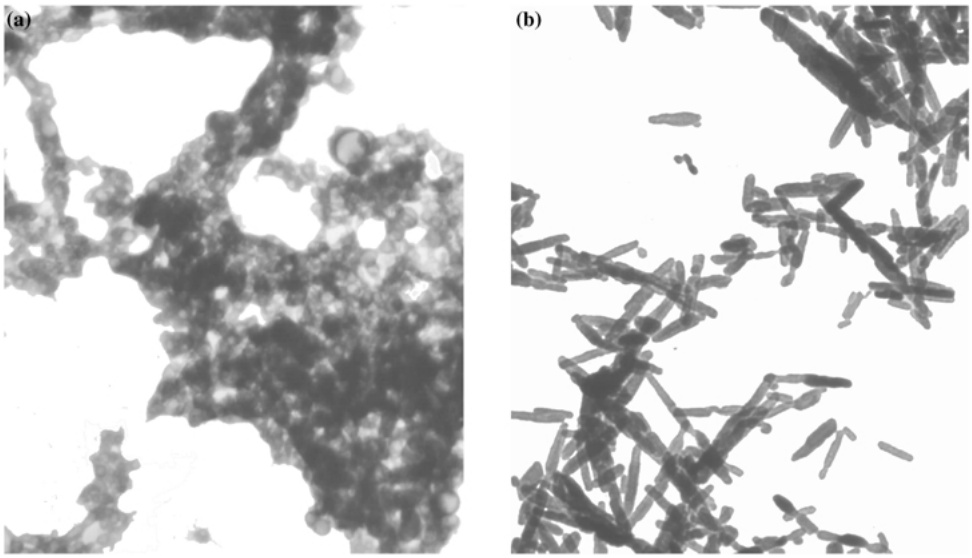

Figure 1 TEM image of HA slurry.

of main peaks of PA66 at 2θ range of 20–24° singificantly decreased. PA66 is the crystalline polymer due to the role of hydrogen bond. In the structure of alpha-PA66, amido and CH_2 methylene chain is on the same plane, the role of NH hydrogen bonds between the molecule chains formed slice-like structure. These H-bond slices arranged along with the main chain consist of the structure of alpha PA66. When PA66 dissolves in the solvent in the compounding process, since the polarity of hydroxyl is stronger than amido, OH of nano-HA on the surface might partly replace NH to form a new hydrogen band with amido in PA66. New hydrogen bonds would affect the plane structure of alpha-PA66, therefore resulted in the decrease of PA66 crystallinity in HA/PA66 composites. This result indicates that nano-HA formed the chemical bond with PA66.

For HA/PA66 composites, the properties of PA66 composed of 50% composite must be crucial to performance of the HA/PA66 composites. To investigate the characteristics of PA66 also, very important are the aspects of the HA/PA66 composites. The XRD patterns at 15–30 of 2θ range were deconvoluted to obtain the crystallinity and the crystalline size and mean lattice strain. The deconvolution software was PEAKFIT (Sigma Company, USA). Fig. 4 shows the deconvolution results of XRD pattern. The number of peaks was determined by second derivative curve of the smoothed XRD experimental data. Table II shows the results of deconvolution of XRD pattern. From the results, the crystallinity of PA66 in composites is significant decrease but the mean crystalline size and lattice strain increase greatly. During the preparation of HA/PA66 composite process, the interaction of HA and PA66 may result in the disorder of PA66 lattice, which produce decrease of PA66 crystallinity. Because of injecting process at 250 °C, the size of PA66 crystals in HA/PA66 composite increases with temperature.

Measurement of mechanical properties

The mechanical properties of the HA/PA66 composites are listed in Table III. Comparing with HA1/PA66 and HA2/PA66 composites, the mechanical performance of HA2/PA66 is better than HA1/PA66. The tensile strength, bending strength and bending modulus of HA2/PA66 are greater than those of pure PA66, but the

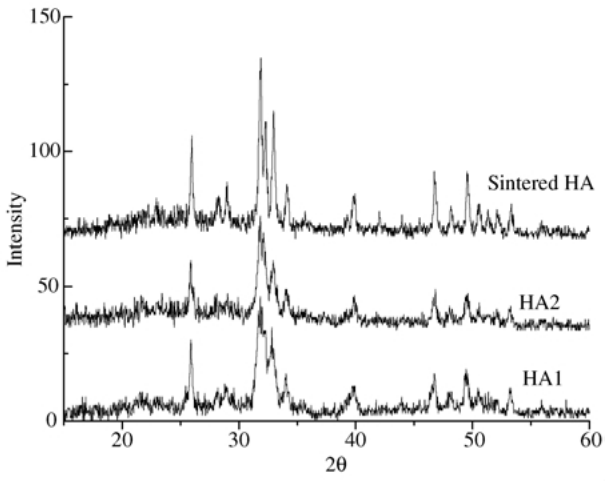

Figure 2 XRD pattern of HA.

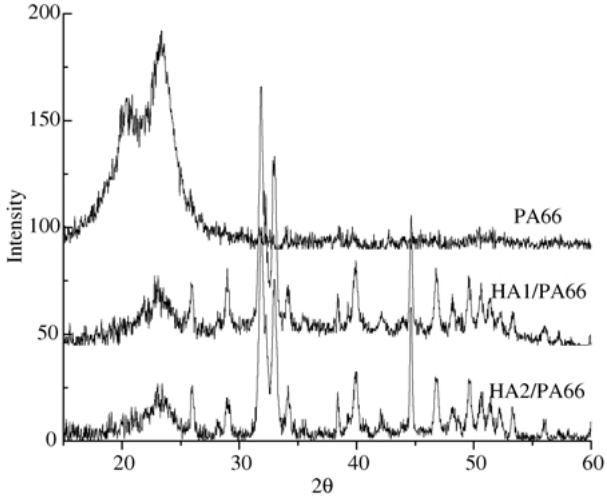

Figure 3 XRD pattern of HA/PA66 composite and PA66.

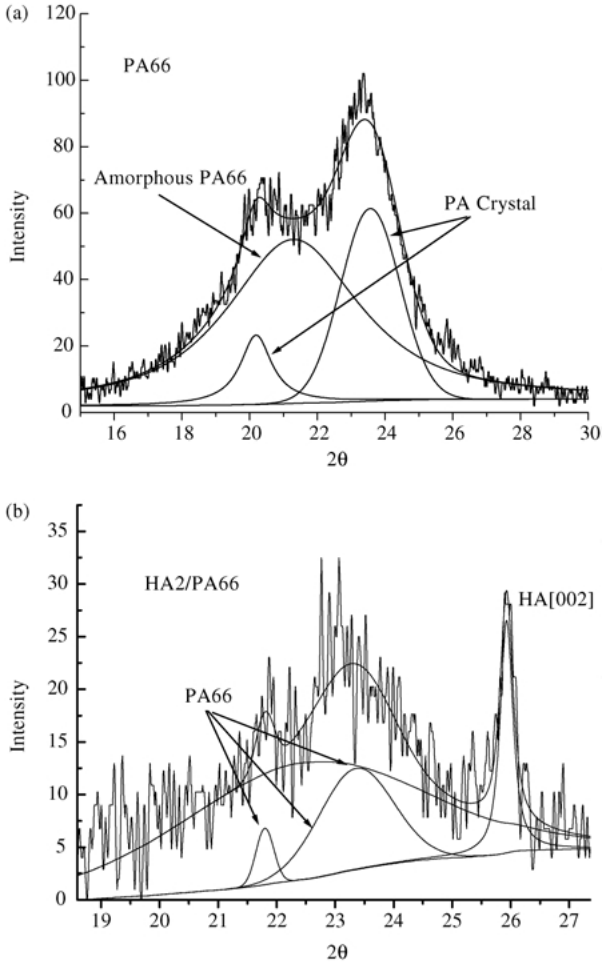

Figure 4 The deconvolution of XRD pattern of (a) pure PA66 and (b) HA2/PA66.

impact strength of HA2/PA66 composite is lower than PA66, i.e. brittleness increases. The mechanical properties for HA2-reinforced PA66 demonstrate that an increase in modulus and strength is achieved at the expense of a decrease in elongation to fracture and an increase of brittleness. The mechanical property of HA1/PA66 is not as good as that of HA2/PA66. The results indicate that nano-HA needle-like crystal is superior in the reinforcing role for PA66 than to that of HA1. The compressive modulus of HA2/PA66 is two times than those of HA1/PA66 and PA. Compared with the bending test, the reinforce effect of HA2 is more obvious during the compressive test. From the HA/HDPE results of Bonfield's [21–22], compressive modulus HA2/PA66 is close with that of HA/HDPE composite (45%HA and 55% HDPE).

SEM analysis of the fracture interface

Fig. 5 is the SEM image of the fracture interface of HA1/PA66 and HA2/PA66. The fracture morphology of HA/PA66 composite exhibits a specific characteristic. In Fig. 4(b), there are no obvious HA2 particles on the HA2/PA66 fracture surface and no interface between HA and PA66 is observed on the fracture. The interface bonding strength of PA66 and HA2 may be strong enough to resist the dissection of phases. The concave and convex morphology appeared on the fracture, which indicated that the fracture of HA2/PA66 is a ductile fracture. On the fracture surface of HA1/PA66 (Fig. 4(a)), the HA1 particles are observed obviously, and it may be caused by the dispersion of the aggregate particles of HA1 floccules. The morphology of the fracture is smoother comparing to HA2/PA66 fracture; the fracture of HA1/PA66 may be a brittle fracture. The fracture interface of both HA/PA66 composites was characteristic of both cohesive and adhesive failure. At the fracture interface of HA1/PA66, the adhesive fracture is more obvious, but cohesive fracture plays more important role in the fracture of HA2/PA66. These results indicate that the reinforcing effect of needle-like nano-HA2 is more obvious than meso-sphere HA1. The analysis of fracture interface agrees with the outputs of the mechanical test.

As regards the weight fraction and distribution of HA in PA66 matrix, the thermal analysis shows that the weight ratio of HA and PA66 is the same as the value prepared (not shown in this paper). From the fracture interface, the HA crystal distributes even in the PA66 matrix, but the HA2 distributed more even than HA1, although both kinds of HA are somewhat aggregated in the PA66 matrix.

Conclusion

It is well known that high weight ratio of HA to PA66 is an essential factor to maintain the bioactivity and the modulus of HA/PA66 composite. In this study, composites with 50/50 weight ratio of HA to PA66 were studied. The high HA : PA66 ratio ensures the composites have better bioactivity. The feature of our synthesis method is that HA slurry was used directly to compound with PA66 in solution. The results of PSD, TEM and XRD showed that the HA particles in HA slurry are nano-apatite crystals. The appearance of some micrometer-scaled particles is due to the aggregate of the nanoparticles. The dispersion of nano-HA slurry is better than the dried or sintered HA powders which often cause firm aggregate between particles in drying and sintering process, the dimension is finer and the specific surface area, i.e. the surface energy, is larger for the nano-HA slurry. All of these properties are suitable for the scattering of the needle-like nano-HA crystals in the PA66 matrix when producing a composite on the nanoscale. The poor crystalline structure of synthesized nano-HA makes it more resorbable, providing higher content of Ca^{2+} and PO_4^{3-} *in vivo* for new bone matrix formation.

TABLE II The characteristics of pure PA66 and PA66 in the composites

	Peak position (2θ)	FWHM (2θ)	Crystallinity (%)	Crystalline size (A)	Mean lattice strain (%)
HA1/PA66	23.287	1.929	28.19	46	4.072
HA2/PA66	23.239	1.499	21.22	60	4.319
PA66	23.565	2.070	32.15	42	3.165

TABLE III The mechanical property date of HA/PA66 composites and PA66

	PA66	HA1/PA66	HA2/PA66
Tensile strength (MPa)	35.7 ± 3.4	39.2 ± 3.6	42.2 ± 4.2
Bending strength (MPa)	70.7 ± 6.8	64.4 ± 5.9	75.3 ± 6.9
Modulus of bend (GPa)	2.20 ± 0.5	5.67 ± 0.9	5.47 ± 0.8
Impact strength (kJ/m^2)	13.70 ± 1.5	4.46 ± 1.2	6.57 ± 0.6
Compressive Modulus (GPa)	1.81 ± 0.86	2.45 ± 0.75	4.89 ± 0.5

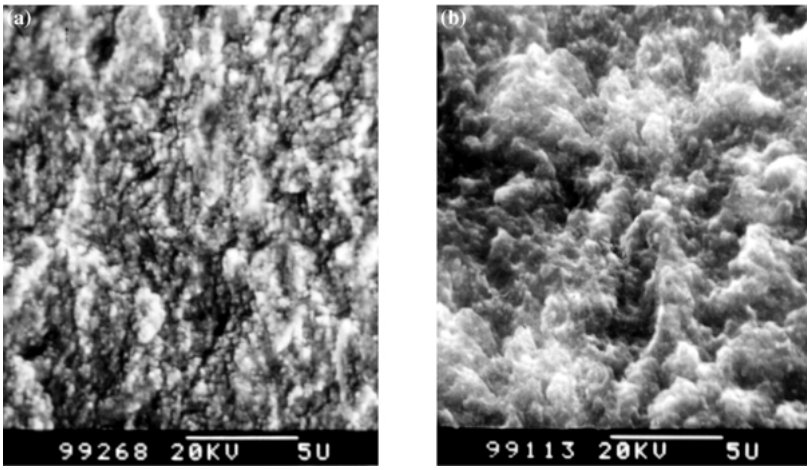

Figure 5 SEM image of fracture interface of HA/PA66 composite (a) HA1/PA66 and (b) HA2/PA66.

From the XRD and SEM analysis it is clearly understood that, due to the role of hydrogen bond, the chemical bond is formed between nano-HA and PA66 in the HA/PA66 composite. As a result, the interface bonding strength between nano-HA needle-like crystals and PA66 matrix is strong and so almost no HA2 particles appeared on the fracture surface of HA2/PA66. On the other hand, since HA2 is the needle-like crystal, it could cross over the interface of micro-crackle in the matrix during the deformation process to overcome the micro-crackle propagation into the cleft and fracture [21]. Therefore, the mechanical property of HA2/PA66 composites is significantly improved. HA1 particles were observed on the fracture surface of HA1/PA66. The fracture may have happened at the aggregate site of HA1 particles, so that the mechanical property of HA1/PA66 composite is lower.

The result indicated that the morphology, crystal structure and crystallinity of nanograde needle-like HA crystals after hydrothermal treatment are similar to those of thin apatite crystal in bone tissues of the body [16, 19]. Nano-HA crystal with needle-like morphology is not only an ideal bioactive filler for polymer composite, but also increases the mechanical properties of HA/PA66 composite. From the structure view, the OH of nano-HA formed the H bond with amido of PA66, the HA/PA66 is a new type of composite other than a mixture. But the research proved that an increase in modulus with weight ratio of HA accompanied a decrease in fracture toughness. Above results indicate that HA/PA66 is a promising bone substitute and further improvement of mechanical properties and optimum weight ratio of HA/PA66 is under investigation.

Reference

1. K. DE GROOT (ed.), ''Bioceramics of Calcium Phosphate'' (CRC Press, Boca Raton, FL, 1983) p. 99.
2. H. AOKI, Science and Medical Application of Hydroxyapatite (JAAS Press, Japan, 1991).
3. M. JARCHO, *Clin. Orthop. Rel. Res.* **157** (1981) 259.
4. T. HANAWA and M. OTA, *Appl. Surface Sci.* **55** (1992) 269.
5. S. P. SOUSA and M. A. BARBOSA, *Clin. Mater.* **14** (1993) 287.
6. W. BONFIELD, J. C. BEHIRI, C. DOYLE, J. BOWMAN and J. ABRAMS, in ''Biomaterials and Biomechanics 1983'', edited by P. Ducheyne, G. Van der Perre and A. E Aubert (Elsevier, 1984) p. 421.
7. Q. LIU, J. R. DE WIJI and C. A. VAN BLITTERSWIJK, Transactions of Fifth World Biomaterials Congress, Toronto, Canada, 1996, **2**, p. 361.
8. Q. LIU, J. R. DE WIJI and C. A. VAN BLITTERSWIJK, Transactions of Fifth World Biomaterials Congress, Toronto, Canada, 1996, **2**, p. 443.
9. C. DOYLE, Z. B. LUKLINSKA, K. E. TANNER and W. BONFIELD, ''Clinical Implant Materials, 1983'', edited by G. Heimke, U. Soltesz and A. J. C. Lee, series *Adv. Biomater.* Elsevier **9** (1990) 339.
10. P. LI, D. BAKKER and C. A. VAN BLITTERSWIJK, *J. Biomater. Mater. Res.* **34** (1997) 79.
11. C. DOYLE, K. E. TANNER, N. ANSEAU and W. BONFIELD, Transactions of Third World Biomaterials Congress, 1988, Vol. 3, p. 469.
12. C. DOYLE, K. E. TANNER and W. BONFIELD, *Biomaterials* **12** (1991) 841.
13. X. L. DONG, ''Essentials of Advanced Materials for High Technology'', edited by H. M. Zeng (Science and Technology Press of China, 1993) p. 561.
14. A. BIGI, G. COJAZZI, S. PANZAVOLTA, A. RIPAMONTI, N. ROVERI, M. ROMANELLO and K. N. SUAREZ, *J. In. Biochem.* **68** (1997) 45.
15. F. H. LIN, C. J. LIAO, K. S. CHEN and J. S. SUN, *Biomaterials* **20** (1999) 475.
16. Y. B. LI, J. DE WIJN, C. P. A. T. KLEIN and S. VAN DE MEER, K. DE GROOT, *J. Mater. Sci. Mater. Med.* **5** (1994) 252.

17. J. Q. FENG, J. X. WANG, Y. B. LI, Y. G. YAN, M. HUANG and X. D. ZHANG, in ''Biomedical Materials Research in Asia (IV)'', edited by Xingdong Zhang and Yooshito Ikada (Kobunshi Kankokai, Kyoto, Japan) p. 77.
18. J. X. WANG, Y. B. LI, J. Q. FENG, Y. G. YAN, M. HUANG and X. D. ZHANG, *High Technol. Lett.* **5** (1999) 103.
19. Y. B. LI, C. P. A. T. KLEIN, J. DE WIJN, S. VAN DE MEER and K. DE GROOT, *J. Mat. Sci. Mater. Med.* **5** (1994) 263.
20. Y. B. LI, K. DE GROOT, J. DE WIJN, C. P. A. T. KLEIN and S. VAN DE MEER, *ibid.* **5** (1994) 326.
21. S. N. NAZHAT, R. JOSEPH, M. WANG, R. SMITH, K. E. TANNER and W. BONFIELD, *ibid.* **11** (2000) 621.
22. M. WANG, C. BERRY, M. BRADEN and W. BONFIELD, *ibid.* **9** (1998) 621.
23. X. S. ZENG, in ''Encyclopedia of Materials Science and Technology'', edited by Changxu Shi (China Encyclopedia Press, Beijing, 1995) p. 1187.

Received 15 August 2000
and accepted 4 February 2003